Contents lists available at ScienceDirect

Atmospheric Environment

journal homepage: www.elsevier.com/locate/atmosenv

Morphological and chemical characterisation of indoor quasi-ultrafine particles

Adobi Okam [a], Paul Sanderson [a], Roy M. Harrison [a,b], Juana Maria Delgado-Saborit [a,c,*]

[a] Division of Environmental Health & Risk Management, School of Geography, Earth & Environmental Sciences, University of Birmingham, Birmingham, United Kingdom
[b] Department of Environmental Sciences, Faculty of Meteorology, Environment and Arid Land Agriculture, King Abdulaziz University, Jeddah, Saudi Arabia
[c] Universitat Jaume I, Perinatal Epidemiology, Environmental Health and Clinical Research, Department of Medicine, Faculty of Health Sciences, Castellon, Spain

HIGHLIGHTS

- Wide range of morphologies found in indoor quasi-Ultrafine Particles (qUFP).
- Average indoor qUFP sizes ranged 35–103 nm and were mainly of irregular shape.
- Si, Fe and S found in qUFP from all indoor locations.
- Indoor qUFP originated from indoor sources, vehicular emissions and soil.
- EDS beam damaged fragile sulphur rich nanoparticles.

GRAPHICAL ABSTRACT
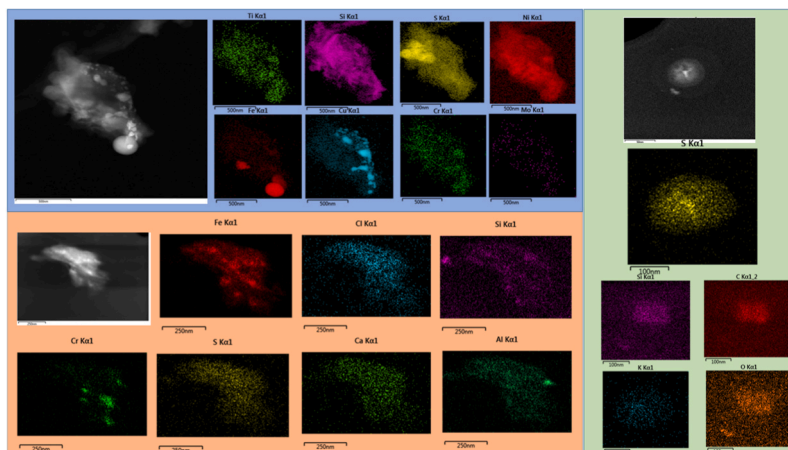
ABSTRACT

Particles in the nanoscale range have intrinsic physicochemical characteristics that define their interaction with the human body and ultimately their toxicity. Whilst research has focused on engineered nanomaterials or ambient ultrafine particles, little is known about the morphology, size and elemental composition of particles in the nanoscale range collected in indoor environments, where humans spend the longest time. This study aims to characterise the physicochemical properties of quasi-ultrafine particles (qUFP), with an aerodynamic diameter <250 nm, collected with a Sioutas impactor from 5 indoor environments (3 homes and 2 offices). Morphology, size and elemental composition of individual particles were imaged using a Transmission Electron Microscope coupled with X-ray energy dispersive spectroscopy. Most of the single particles and their aggregates were of irregular shapes, and some fibrous rods, elongated rods, spheres and hexagons were also observed. ImageJ software was used to analyse the surface area, roundness and circularity of the particles, as well as individual particle diameter for the spherical particles. For the non-spherical shaped particle, the particles were manually measured to characterise the maximum Feret diameter. Particle main dimensions (i.e. diameter for spheroids and maximum Feret diameter for irregular particles) ranged from 35 ± 59 nm to 103 ± 160 nm. Shapes for non-spherical particles were assigned by visual description. Si, Fe and S were found in nanoparticles from all indoor locations. Other abundant constituents were K, Cr, Na, Ca, Cl found in 60–80% of locations. Minor constituents of indoor nanoparticles were Cu, Sn, Ti, Mo, Al, P, Be, F, Zn, Rb, Pb, Mn and Co. Sources were related to indoor emissions, e.g.

printers, stainless-steel tools, electronics, cooking, house chores, particle re-suspension, aerosol and cleaning products as well as to penetration of outdoor nanoparticles from vehicular emissions, soil and secondary aerosols. Detailed investigation of the physicochemical properties of these particles can help understand their associated hazard and their fate in the human body.

1. Introduction

Airborne Particulate Matter (PM) is a heterogeneous mixture of various substances with different shapes and sizes ranging from a few nanometres to tens of micrometres. Research has shown that nanosized particles can have properties intrinsic to their size that are not shared by large particles or by particles with the same bulk chemical composition (Auffan et al., 2009; Handy et al., 2008).

PM can be generated from combustion and non-combustion sources (Pope and Dockery, 2006). Particles in the ultrafine fraction can be formed through nucleation, gas to particle reactions, evaporation of larger particles, or during incomplete fuel combustion (Brouwer et al., 2004; Li et al., 2003). Ultrafine particles (UFP) are being generated continuously and in large numbers by both natural and anthropogenic sources present in the urban and rural areas as well as in indoor environments.

Recent studies focusing on the indoor environment have suggested that personal exposure in a non-smoking suburban indoor environment can be similar or higher than exposures outdoors (Wallace and Ott, 2011). Indoor airborne particles may arise from indoor sources such as cooking (Dennekamp et al., 2001; Shehab et al., 2021), other combustion sources (e.g., smoking, gas heaters, use of candles, oil lamps and incense) (Vu et al., 2017a), use of consumer products that produce aerosol (e.g. sprays and cleaning products) (Fromme, 2012; Ogulei et al., 2006; Vu et al., 2017a) and cleaning activities (e.g. dusting, vacuum cleaning) (Vu et al., 2017a). In office environments, nanosize particles are emitted from printers and photocopiers (Khatri et al., 2013). Other sources of indoor particles include penetration from the outdoors (which can be removed by deposition, adsorption, and other mechanisms), from appliances that are operated by electric motors and re-suspension of particulate matter from house dust by humans and pets (Fromme, 2012; Hänninen et al., 2004; Ogulei et al., 2006; Szymczak et al., 2007; Wallace and Ott, 2011). The morphology and elemental composition of particles provide information on their characteristics and sources (Kang et al., 2009).

UFPs are increasingly studied because they have been considered to be associated with adverse health effects. Exposure to UFP has been associated with respiratory effects, ability to generate oxidative stress and inflammation to the lungs (Oberdörster et al., 2005b; Pope, 2000), as well as with cardiovascular (Araujo et al., 2008; Donaldson et al., 2001), metabolic (Stewart et al., 2010), neurological (Heusinkveld et al., 2016) and reproductive systems (Campagnolo et al., 2012; Hou and Zhu, 2017; Wing et al., 2020). Characteristics of nanosized materials influence their fate and behaviour in the environment and their potential to induce toxicity in human and different environmental receptors (Stone et al., 2010). Therefore, whilst the main property to define toxicity in the assessment of toxicity of bulk particles mainly relies on dose (Oberdörster et al., 2005a), in the case of UFP, physicochemical properties such as size, shape and chemical composition of nanosized particles might be important parameters to consider when assessing their toxicity (Gatoo et al., 2014). For example, a study by Renwick et al. (2004) showed that ultrafine BC and TiO_2 particles administered to rats, induced inflammation and epithelia damages to a greater extent than their bulk particle counterpart (Renwick et al., 2004). Similarly, a study comparing silver wires and spherical particles found that wires strongly affected alveolar epithelial cells, whereas spherical particles showed no effect (Stoehr et al., 2011).

People spend about 85–93 % of their time indoors (Delgado-Saborit et al., 2011; Höppe and Martinac, 1998; Lazaridis, 2011; Okam, 2017), as such indoors contribute a significant amount to PM exposure

(Delgado-Saborit, 2019; Vinzents et al., 2005). It is now widely recognized that a significant proportion of personal exposure to particles occurs in the indoor environment (Delgado-Saborit, 2019). Indoor PM are characterised by chemical compounds of which some could be toxic. In a study by Long et al. (2001), rat alveolar macrophages (AMs) treated with either indoor or outdoor $PM_{2.5}$ released significant amounts of tumour necrosis factor (TNF) compared to control AMs. However, a comparison of paired indoor/outdoor data in that study reported significantly greater TNF releases elicited by indoor $PM_{2.5}$ samples than by the corresponding outdoor samples (Long et al., 2001). As such, Long et al. (2001) suggested that some particles of indoor sources may be more bioactive than the particles of outdoor origin in his experiment (Long et al., 2001).

Over the past decade, indoor studies on particle concentration levels, size distribution, and source contribution have received increased attention (Ali et al., 2022; Diapouli et al., 2013; Manigrasso et al., 2019; Marval and Tronville, 2022; Morawska et al., 2017; Vardoulakis et al., 2020; Zhang et al., 2021). The toxicity of particles will likely differ depending on their characteristics such as size, shape, and chemistry (Albanese et al., 2012). However, only few studies have carried out physicochemical characterisation of indoor particles (Arora and Jain, 2015; Glytsos et al., 2010; Pipal et al., 2021; Vu et al., 2017a). In addition, information on the physicochemical properties of UFP typically found in indoor environments is required to guide the design of toxicological studies that investigate potential toxic effects associated with indoor particles. Therefore, to protect people against the possible risk associated from inhalation of ultrafine particles found in indoor environments, the physical and chemical properties of these particles need to be characterised so their toxicity can be investigated.

This study aims to characterise the physicochemical signatures of indoor particles typically found in the nanosized range that could inform future studies to evaluate their toxicity. For that purpose, we characterised the size, morphology and surface chemical composition of quasi-ultrafine particles (<0.25 μm in diameter, qUFP) collected from several indoor environments, such as homes and offices, using a Transmission Electron Microscope (TEM) coupled with X-ray energy dispersive spectroscopy (EDS).

2. Method

2.1. Sample location

Indoor quasi-ultrafine particles were collected from three homes and two offices in Birmingham, a major city in the United Kingdom, with circa of 1,2 million inhabitants according to the 2021 census estimate,[1] and 3.8 million inhabitants in the wider Birmingham Metropolitan area.[2]

Home 1 and Home 2 are located in a suburban area, about 1.5 miles from Birmingham (UK) city centre, while Home 3 is about 0.8 miles from Birmingham city centre, in an urban area. Home 1 and Home 2 are in a residential area, while Home 3 is located in a mixed commercial and residential area. That is, Home 3 has heavy mixture of residential and commercial buildings (restaurants, shops) and the Worcester and Birmingham Canal is in very close proximity. The sampler during sampling was placed in the living room for all three homes. Home 1 and Home 2

---

[1] https://www.birmingham.gov.uk/info/20057/about_birmingham/1294/population_and_census.

[2] https://populationdata.org.uk/population-of-birmingham/.

are single occupant homes while Home 3 housed two adults.

Office 1 and Office 2 are both in the Geography building in the University of Birmingham. Office 1 is located on the third floor, facing a low traffic road and car park of about 10–12 cars. While Office 2, the Map Room and photocopying room, is located on the ground floor by the entrance of the building with a grass and flower area in front of the window. During sampling, nobody was present in Office 1 and the windows were open. Office 2, had windows open and normal activity such as photocopying and people movement were ongoing during sampling.

Ethical approval was granted by the Humanities and Social Sciences Ethical Review Committee of the University of Birmingham (ERN_12-0569).

2.2. Sample collection

qUFPs were collected for analysis using Transmission Electron Microscope (TEM) grids (3 mm holey Carbon Films 300 mesh on nickel, Agar Scientific) mounted onto the PTFE filter by using a tiny streak of adhesive at two opposite ends. The filters with the TEM grids attached (Hammer et al., 2021) were placed on the impactor stages of a Sioutas Cascade Impactor operating under normal conditions (9 LPM). The TEM samples have aerodynamic diameters as they were collected using the Sioutas impactor for the five stages representing the five size fractions >2.5, 1.0–2.5, 0.50–1.0, 0.25–0.50 and <0.25 μm. However, only TEM grids located on the <0.25 μm size fraction, representing the quasi-ultrafine fraction, were analysed for this study.

TEM samples were collected between June and November 2014 from 3 homes from subjects participating in the FABLE project,[3] and from 2 workplaces within the School of Geography, Earth and Environmental Sciences of the University of Birmingham. The houses were selected by convenience among those participants who allowed the researcher to sample for a period of time of 1–3 h. Samples were collected as follows:

a) The first TEM sample was collected for 4 h at a subject's home whilst the subject performed various indoor activities, including cooking for 1 h.
b) The second TEM sample was collected for 1 h in a home whilst the subject performed various activities.
c) The third TEM sample was collected for 2 h from another subject's house, where the subject did not perform any particular indoor activity.
d) Two sets of TEM samples were collected for 2 h from two different offices

The sampling time was reduced from 4 h to 1 h between the first and second sample because the TEM grid collected in the first house was heavily loaded (i.e. particles collecting on top of each other) making it difficult to conduct TEM analysis of individual particles. Upon inspection of the second TEM sample, few particles were found. Hence, it was decided to increase the collection time to 2 h. Upon inspection of the subsequent samples collected during 2 h, it was found that 2 h was the ideal sampling time to avoid over/under loading the TEM grid. Despite the different sampling times, all 5 sets of samples were analysed and findings are presented since the different collection time doesn't affect the physicochemical characteristics of the particles under investigation and all samples collected offer useful insights.

2.3. Sample analysis

The size, morphology and surface chemistry for the particles collected on the <0.25 μm size fraction of the Sioutas impactor were imaged using a TEM coupled with X-ray energy dispersive spectroscopy

---

(EDS) (TEM/EDS). Almost all particles on the TEM grid were viewed but only a few representative examples are presented in this paper. The displayed representatives in this paper were chosen because they are the predominant shapes, chemistry or particles that were observed to be unique. The viewed particles were analysed using imageJ.

TEM imaging

Imaging of samples was carried out using a Tecnai F20 TEM working on high tension at 200 kV, with an extraction voltage of 4450 V. Bright-field particle imaging in TEM mode was carried out using the GATAN digital micrograph attached to the instrument to characterise physical properties. In the case of chemical properties characterisation, the instruments STEM mode was used in conjunction with high angle annular dark field (HAADF) detection for identifying likely particles and carrying out EDX analysis (Sanderson et al., 2016).

Physical properties

Physical properties were characterised by circularity, determined by ImageJ software, and by manual measurement of the maximum Feret diameter for non-spherical shapes as described in detail in the Supporting Material.

Chemical properties

Single particle chemical analysis was carried out using x-ray energy dispersive spectroscopy (X-EDS or EDX) as described in detail in the Supporting Material.

3. Results and discussion

3.1. Description of physicochemical properties of indoor particles

This study aimed to characterise the physicochemical properties of quasi-ultrafine particles collected from indoor environments (home and work place). Simultaneous collection of bright field and dark field images of the same particles proved to be difficult. Finding the particles again while switching between modes was not straightforward; and identifying the same particle in the two modes was challenging owing to the different physico-chemical features emphasised in each mode (Sanderson, 2015). Therefore, physical properties were characterised in bright-field particle imaging mode, whereas chemical properties were characterised using dark-field images.

The assessment of the various TEM particle images suggests that most of the particles existed as aggregates of primary particles (PPs). Particles rarely existed as single metallic particles. Morphologically, most of the particles were "shapeless" (irregular), not spherical, and generally particles were mixed with carbon, consistent with other studies (Adachi and Buseck, 2008; Chithra and Nagendra, 2013). In viewing the results, it should be borne in mind that much of the mass of $PM_{2.5}$, including the qUFP (<250 nm) fraction, comprises semivolatile components, most notably ammonium nitrate and much of the organic matter. This will be lost in the vacuum of the TEM, together with some other constituents such as ammonium sulphate, not normally regarded as semi-volatile, but likely to be volatilised at the high energy of the electron beam.

The particles observed in this TEM analysis were mostly in 5 shapes; 1) Irregular and aggregates of irregular shapes consistent with other studies (Adachi and Buseck, 2008; Geng et al., 2010; Maskey et al., 2012; Zhang et al., 2018); 2) Fibrous rod in line with others (Geng et al., 2010; Zhang et al., 2018); 3) Sphere and aggregates of spheres consistent with (Adachi and Buseck, 2008; Chithra and Nagendra, 2013; Geng et al., 2010; Maskey et al., 2012; Zhang et al., 2018); 4) Hexagon; and 5) Rods in line with others (Geng et al., 2010). Shapes were assigned by visual description and comparison to other studies. Table 1 show the total number particles and frequency of shape observed per site. For all the sites, mostly irregular shapes were observed and this has been seen in other studies conducted outdoors (Adachi and Buseck, 2008).

Table 1

Diameter, number of particles and frequency[a], bracket, of the total number of particle shapes counted per each site.

Shape/location	Diameter (nm)	Irregular and aggregates of irregular shapes	Fibrous rod	Sphere and aggregates of spheres	Hexagon	Rod	Total particle numbers counted per site
Home 1	39 ± 102	209 (61.8%)	1 (0.3%)	104 (30.8%)	1 (0.29%)	23 (6.8%)	338
Home 2	93 ± 86	21 (87.5%)	–	1 (4.2%)	2 (8.3%)	–	24
Home 3	61 ± 70	170 (90.4%)	–	18 (9.6%)	–	–	188
Office 1	35 ± 59	61 (81.3%)	–	11 (14.7%)	–	3 (4.0%)	75
Office 2	103 ± 160	43 (87.8%)	–	2 (4.1%)	–	4 (8.2%)	49

[a] Frequency of observation of shape per site (%), - = Shape not observed.

3.1.1. Shape and surface chemistry for particles collected at home 1

Fig. 1 show the different shapes of particles found in Home 1 in the filter representing the qUFP. This includes agglomerates of PPs, spheres, hexagon, rods, irregular shapes, Fig. 2 shows the elemental map surface chemistry constituents of the agglomerate (Fig. 1a). Despite the TEM grid being made of Ni, the elemental map shows that this agglomerate contains Ni, since the Ni map clearly defines the contour of the agglomerate. The PPs in Fig. 1a are more clearly defined compared to other particles observed in the TEM grids. This agglomerate has an average diameter of 112 nm. Fig. 2 shows that this agglomerate contains Cr, Fe and Ti (in addition to Ni) possibly from the same source, since they appear to be dispersed in a similar manner. This is indicative of the same source, possibly stainless steel (Li et al., 2015), according to scientific evidence summarised in Table 3. Stainless steel is the preferred material employed in cooking utensils used in homes and also stainless steel is used for working surfaces and other building materials in the home. Cr is a component of stainless steel and stainless materials are used in many home utensils (Taner et al., 2013).

In addition to Cr, Fe, Ni, these particles contained other alloying elements added to enhance the structure and properties of stainless steel, including Ti, Cu and Mo (Li et al., 2015).

The morphology of the particle presented in Fig. 1a is an agglomerate of irregular shapes. In addition, particle shown in Fig. 1 contains S, which could imply it originates from a combustion source (Viana et al., 2008). It could also be that the S coagulated with or condensed onto the agglomerate. The agglomerate also contains Si, which could originate from soil or road dust adhered to the particle (Viana et al., 2008). On the other hand, other particles with a morphology very similar to soot were observed in Home 2 (Figure S9). The particles found in Home 2 similar to soot only contain C and O, consistent with the chemical composition of black carbon (Hu et al., 2021).

All the different shapes of particles observed in Home 1 (see Fig. 1 (a – f) showed similar chemical composition with the only variation being the percentage of the different elements in each particle. This shows that the particles are likely from the same source/activity. In Home 1, the main activity during sampling was cooking for 1 h.

The particle presented in Fig. 1c is sensitive to the electron beam as shown in Fig. 3. After the image of the particle was taken (Fig. 3a), three
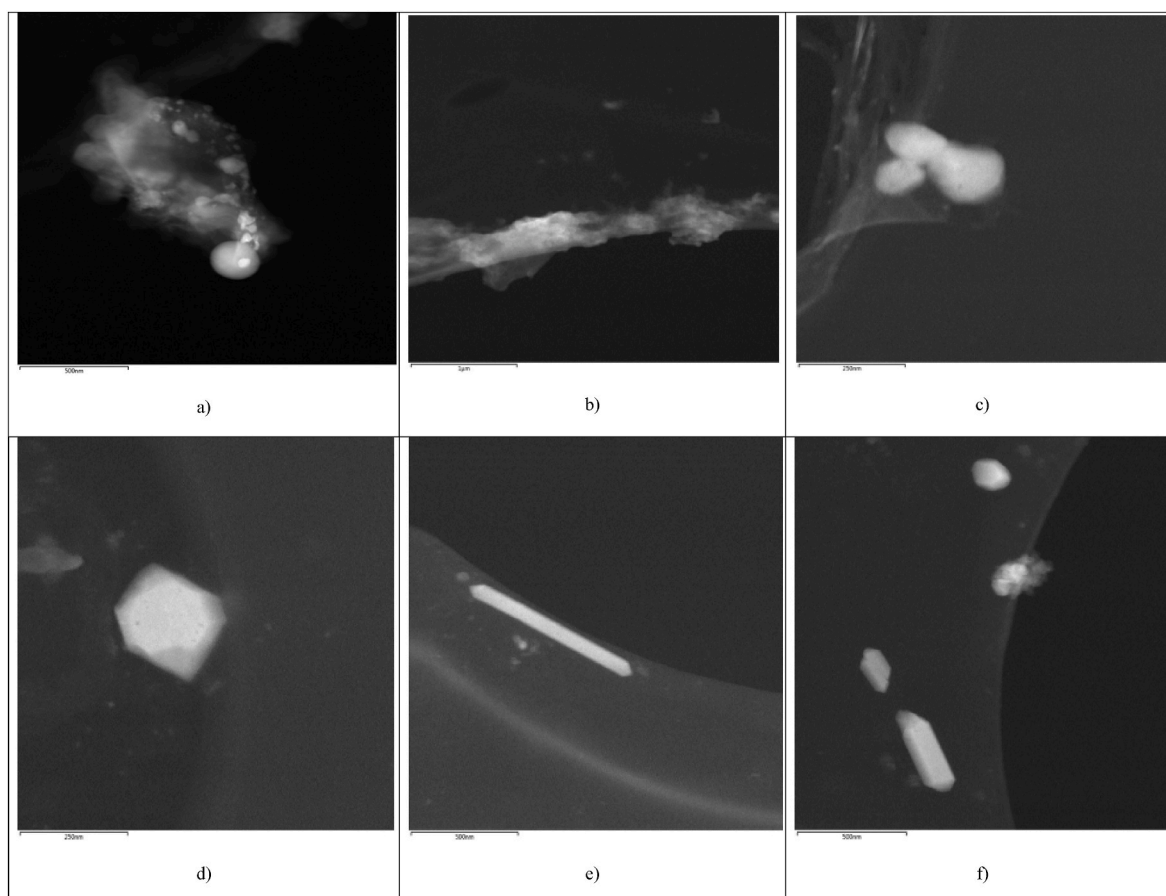
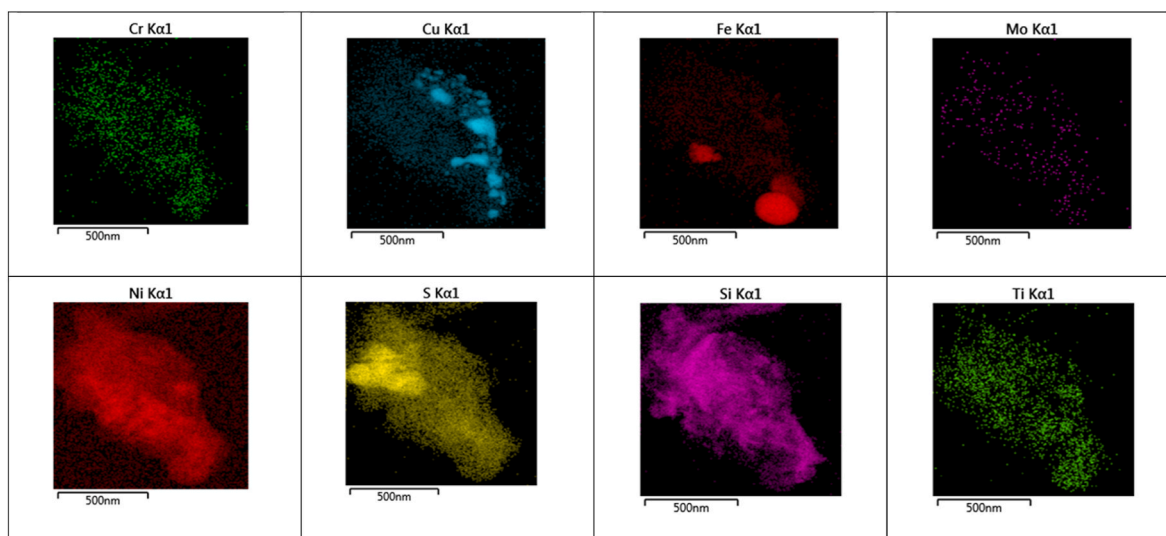**Fig. 1.** Dark field images of particles found in Home 1.

Fig. 2. Elemental map of particle (Fig. 1a) found in Home 1.

areas of the particle were subjected to EDS characterisation (Fig. 3b). This resulted in damage to the particle from evaporation of some constituents of the particle, mainly sulphur and to a much lesser extent nickel (likely a constituent from the TEM grid), within few seconds under the strong electron beam used to perform the EDS analysis. As shown in the temporal sequence of the images taken and displayed in Fig. 3a–c, three squares are observed on the particle (Fig. 3c) on the exact same locations where the three spectra were previously collected (Fig. 3b). This particle is composed mainly of sulphur as shown in Fig. 3 and Figure S2. Damage to fragile particles imaged and characterised with a TEM has been reported previously, especially for organic compound and salts (Ott et al., 2021). Researchers have also identified particles containing sulphate that present a similar behaviour under the strong beam of the TEM (Maskey et al., 2012; Toyokuni, 1999). The particle EDS elemental map shows the evaporation or depletion outlined on the sulphur and this is not evident in the other elements, apart from nickel to a lesser extent (Fig. 3). Nickel is a constituent of the TEM grid (Fig. 3j). As observed in Fig. 3, the strong beam has damaged the integrity of the particle and this can be said to be one of the disadvantages of using electron beams for imaging. Other particles that were sensitive to the electron beam were also observed, which also showed high average composition of S in them. Adachi and Buseck (2008) suggested that organic material particles were more stable to the electron beam than S-rich particles (Adachi and Buseck, 2008). Maskey et al. (2012) suggested that these particles that evaporate under the electron beam are regarded as mixtures of semi and/or less volatile organic species and ammonium sulphate/bisulphate (Maskey et al., 2012). Geng et al. (2010) suggested that ambient soot particles which have been processed for few hours are heavily internally mixed, primarily with ammonium sulphate (Geng et al., 2010). Particles that contain these sulphates could originate from outdoor sources, such as traffic, industry or secondary aerosols (Viana et al., 2008) infiltrating into the indoors.

Ca and Si particle contribution were 42 % and 18% respectively in Home 1 (Table 2). In Home 3 and Office 1 no Ca particles were observed. Home 2 and Office 2 had high contribution of Si (31 % and 18 % respectively) and the Ca contribution for both were 3.1 % and 8.2 % respectively. The Ca-rich and Si-rich particles observed in Home 1 could be associated with cooking emissions, because they were found mostly in Home 1, and this was the only home where cooking activities were undertaken during sampling. Ca-rich qUFP could arise from aerosol production when boiling hard water (Hankin et al., 1970; Sengupta, 2013). Additionally, Ca could also originate from the ingredients. In a study on morphology and characteristics of PM in a Chinese restaurant,

it was observed that in contrast to other PM sources, the PM emitted from cooking primarily consisted of Ca-rich, C-rich, and Si-rich particles (Li et al., 2019). Even though the cooking activity during our sampling was not a Chinese style cooking, we observed similar pattern of high content of Ca and Si qUFP (C contribution was not measured in this study). This is consistent with a study that reported that approximately 4–79 % of the calcium content of different ingredients can be lost during cooking, mainly during boiling (Kimura and Itokawa, 1990). Similarly, another study found that using bones for cooking increased the content of calcium in chicken soup (Rosen et al., 1994). These losses are consequence of the leaching of calcium and other minerals from the ingredients (e.g. meats and vegetables) to the broth during cooking, occurring in cooking processes involving water, such as steaming and boiling (Gerber et al., 2009). Therefore, it is plausible that the calcium leached from the ingredients into the broth could be aerosolised during cooking and subsequently captured in the filters.

3.1.2. Shape and surface chemistry for particles collected at home 2

Fig. 4 presents an agglomerate particle containing Cl, Al, Ca, Si, which are elements found in soil and are usually of mineral origin (Viana et al., 2008). Since the maps of all these compounds are very similar, this agglomerate is suggested to be clay of mineral origin. However, the main element found in the particles collected in this Home is Fe (34%) whereas the Cl makes up only 1.4% of the total elemental contribution (Table 2).

3.1.3. Shape and surface chemistry for particles collected at home 3

Fig. 5 shows a particle made up of O, Fe and Cr indicating that the particle is an oxide of Fe or oxide of Cr. Most probably, this particle is a rust particle as rust exists most commonly as oxides of Fe.

3.1.4. Shape and surface chemistry for particles collected at office 1

Fig. 6 shows a doughnut shaped like particle and its elemental map collected from office 1. The elemental map indicates that this particle contains a mixture of S, Na, K, Si, C and O. It has the similarities of the doughnut shaped particle described by (Maskey et al., 2012). In their study, this particle was collected from the ambient air and the source was associated with biomass burning from a nearby agricultural area. In our study, the particle shown in Fig. 6 was collected indoors and also has Si as part of the surface chemistry. The Si in combination with the Na and K found suggest soil origin but also could be from combustion origin because of the S and C content.

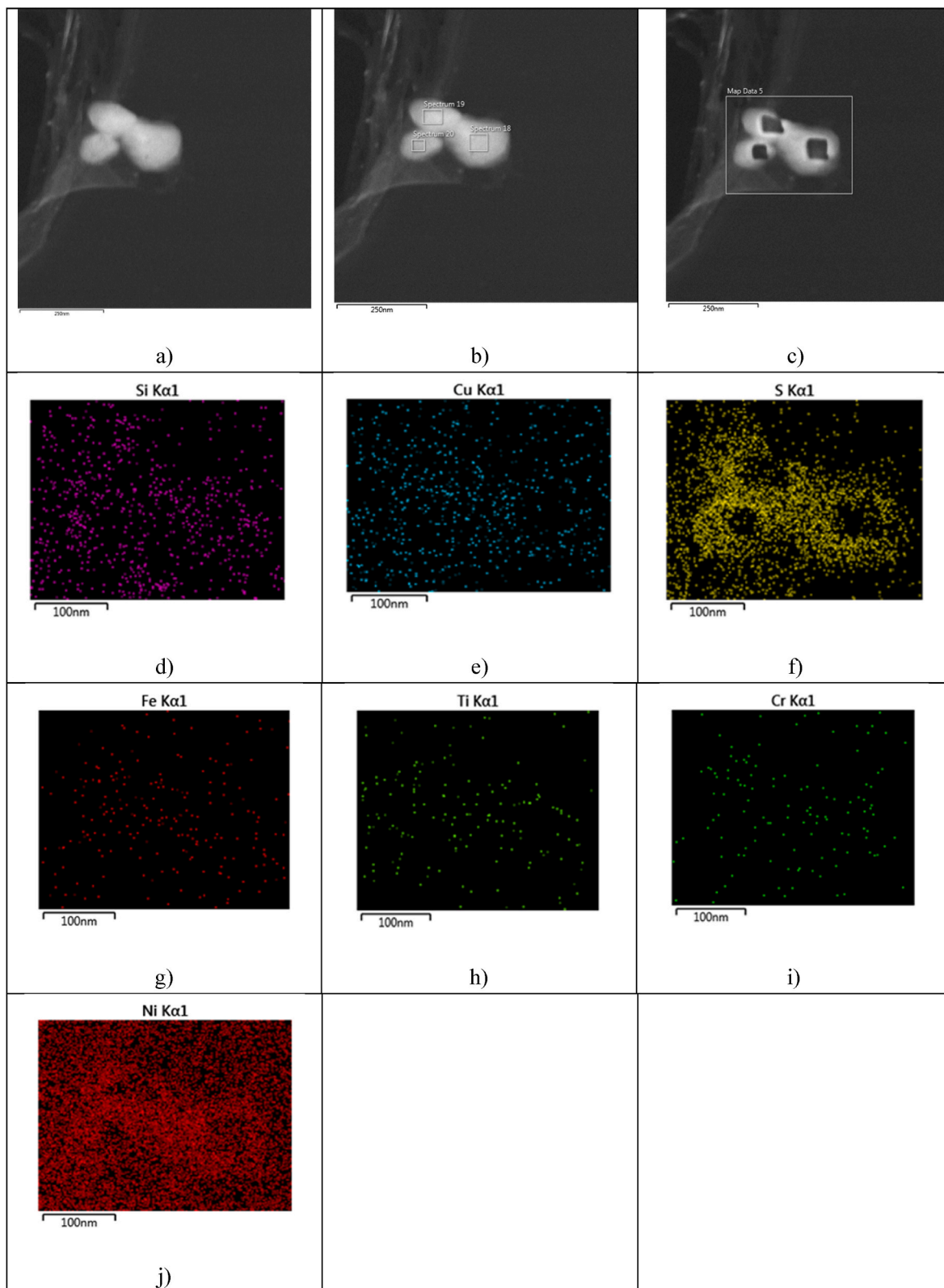Fig. 7 shows another particle aggregate collected from Office 1. The

Fig. 3. Dark field images (a–c) EDS map (d–i) for particle and TEM grid (j) shown in Fig. 1c found in Home 1. Fig. 3b) shows the locations where 3 spectra were analysed. Fig. 3c) shows damage to the particle from the EDS beam. Fig. 3f) shows evaporation of sulphur in the particle damaged by the EDX beam. Fig. 3i) shows evaporation of nickel (to a much lesser extent) in the particle damaged by the EDX beam.

Table 2
Elemental average relative contribution to spectra, relative contribution of elemental spectra per microenvironment and frequency of occurrence of elemental spectra in microenvironment characterised.

Elements	Home 1 (43 particles)		Home 2 (10 particles)		Home 3 (12 particles)		Office 1 (12 particles)		Office 2 (18 particles)		Frequency (%)
	Average Weight ± Standard Deviation (N)	% Contribution	Average Weight ± Standard Deviation (N)	% Contribution	Average Weight ± Standard Deviation (N)	% Contribution	Average Weight ± Standard Deviation (N)	% Contribution	Average Weight ± Standard Deviation (N)	% Contribution	
Si	26 ± 32 (43)	18	40 ± 44 (8)	31	46 ± 38 (7)	17	58 ± 37 (10)	39	50 ± 47 (10)	18	100
Fe	4.8 ± 18 (43)	3.4	44 ± 28 (4)	34	63 (1)	24	30 ± 24 (5)	20	74 ± 15 (3)	26	100
S	27 ± 22 (43)	19	12 ± 15 (6)	9.2	62 ± 36 (6)	23	16 ± 16 (8)	11	29 ± 12 (10)	10	100
K	6.1 (1)	4.3	0.5 (1)	0.4	59 ± 29 (4)	22			44 ± 32 (13)	16	80
Cr	0.7 ± 3.3 (43)	0.5	7.1 ± 7.9 (4)	5.4	15 (1)	6			15 (1)	5.4	80
Na			16 ± 21 (2)	12	20 (1)	8	3.78 ± 2.7 (3)	2.5	23 ± 5.7 (4)	8.2	80
Ca	59 ± 25 (20)	42	4.0 ± 5.8 (4)	3.1					23 ± 17 (2)	8.2	60
Cl			1.8 ± 1.4 (3)	1.4			1.3 (1)	0.9	18 ± 26 (3)	6.4	60
Cu	7.9 ± 18 (43)	5.6	1.7 ± 0.3 (2)	1.3							40
Sn	5.2 (1)	3.7									20
Ti	0.8 ± 2.9 (43)	0.6									20
Mo	3.37 ± 13.44 (25)	2.4									20
Al			2.5 ± 1.5 (4)	1.9							20
P			0.9 ± 0.3 (3)	0.7							20
F							2.7 (1)	1.8			20
Zn							0.8 ± 0.3 (2)	0.5			20
Rb							3.0 (1)	2.0			20
Pb							34 ± 9.3 (3)	23			20
Mn									3.3 (1)	1.2	20
Co									0.22 (1)	0.08	20

Total number of particles analysed in each site are Home 1: 43, Home 2: 10, Home 3: 12, Office 1: 13 and Office 2: 18. (N) = number of particles per site that their elemental composition/spectra were observed.
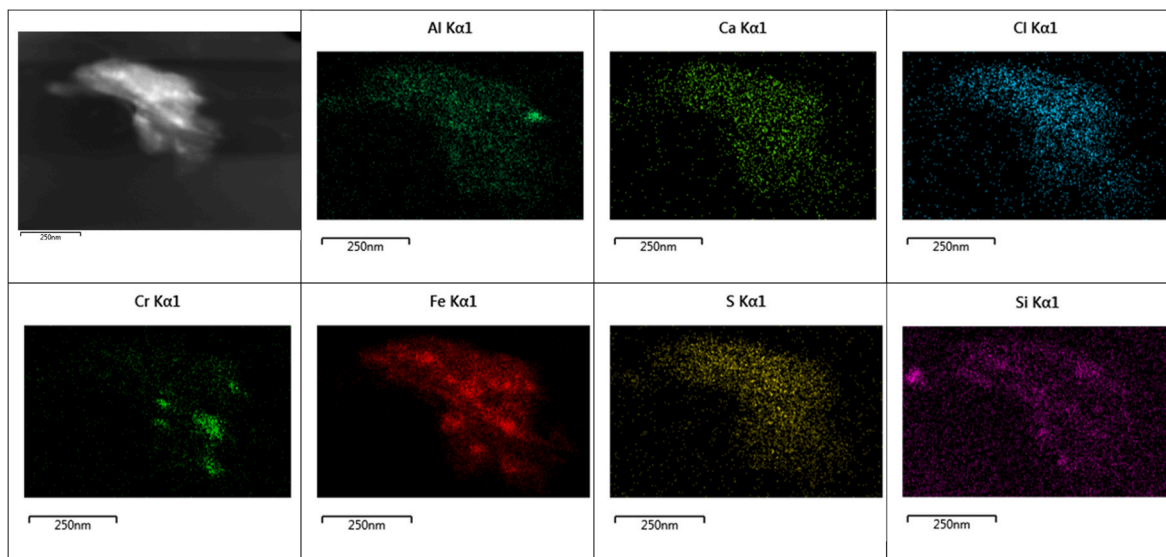

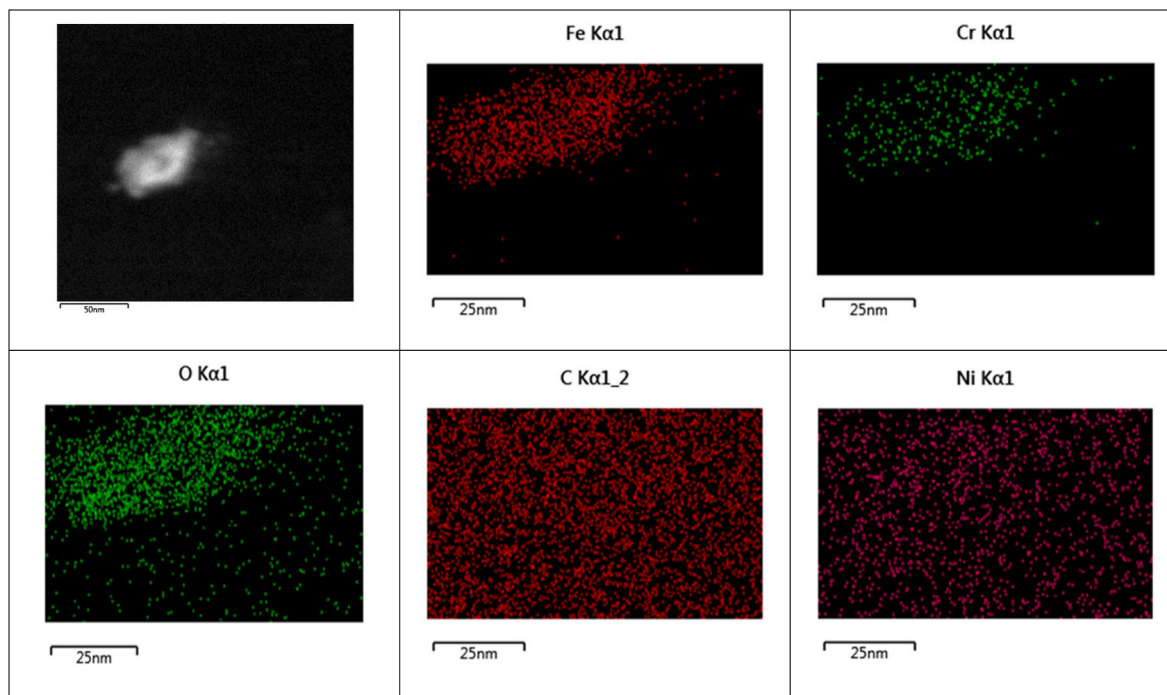**Fig. 4.** Dark field image and elemental map of particle found in Home 2.

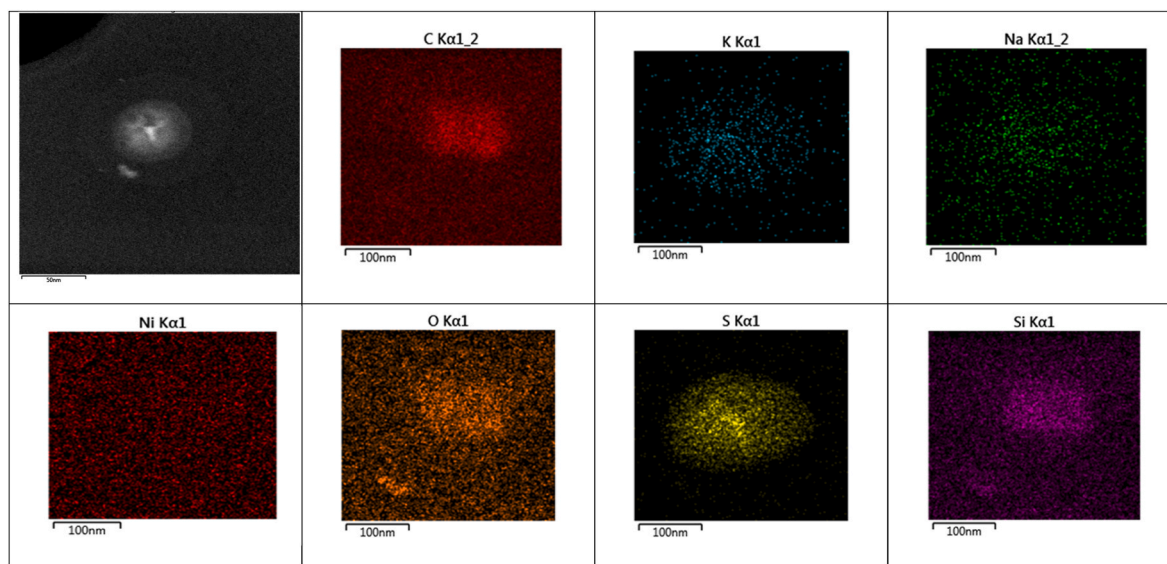**Fig. 5.** Dark field image and elemental map of particle found in Home 3.

Fig. 6. Dark field image and elemental map of particle found in Office 1.

morphology and elemental composition of this agglomerate suggest that is from a mixed source: combustion, road dust, mineral and soil source. Its elemental map (Fig. 7) shows it is rich in S, K, C and O, indicating combustion, whereas the Pb, Ni, Rb and Fe suggests road dust origin (Pant and Harrison, 2013). Office 1 windows were open and the window faced a minor road and a car park (that parks about 10–12 cars) with a grassy area within the campus of the University of Birmingham, with a water canal not too far away. The Cl and the Na could be from clay minerals. While the Na indicates a crustal origin (Chithra and Nagendra, 2013). This particle also contained F.

3.1.5. Shape and surface chemistry for particles collected at office 2

Fig. 8 shows an aggregate collected from Office 2. This office also known as the Map Room, holds a collection of maps and is a room where printing and photocopying activities takes place. Most of the particles observed were in the form of aggregates thereby making the primary particles less obvious. Fig. 8 show that this particle is an aggregate of a mixture of different elements, including Ca, Co, Cr, Fe, K, Mn, Ni and Si. The sources of the elements found in this aggregate could include metals found in printer toners Ni, Mn, Fe and Si (Martin et al., 2015). Ca and Mg are constituents of paper (Martin et al., 2015). This particle also contains Co, which could be a constituent of ink used in the photocopier and printers (Brown et al., 2018). This is consistent with the main activity of the room storing paper maps, books and photocopying activity. This office is also located in the ground floor overlooking a grassy area, which is consistent with the aggregate containing Ca, K, Mg, Si and Fe, which could be attributed to crustal origin.
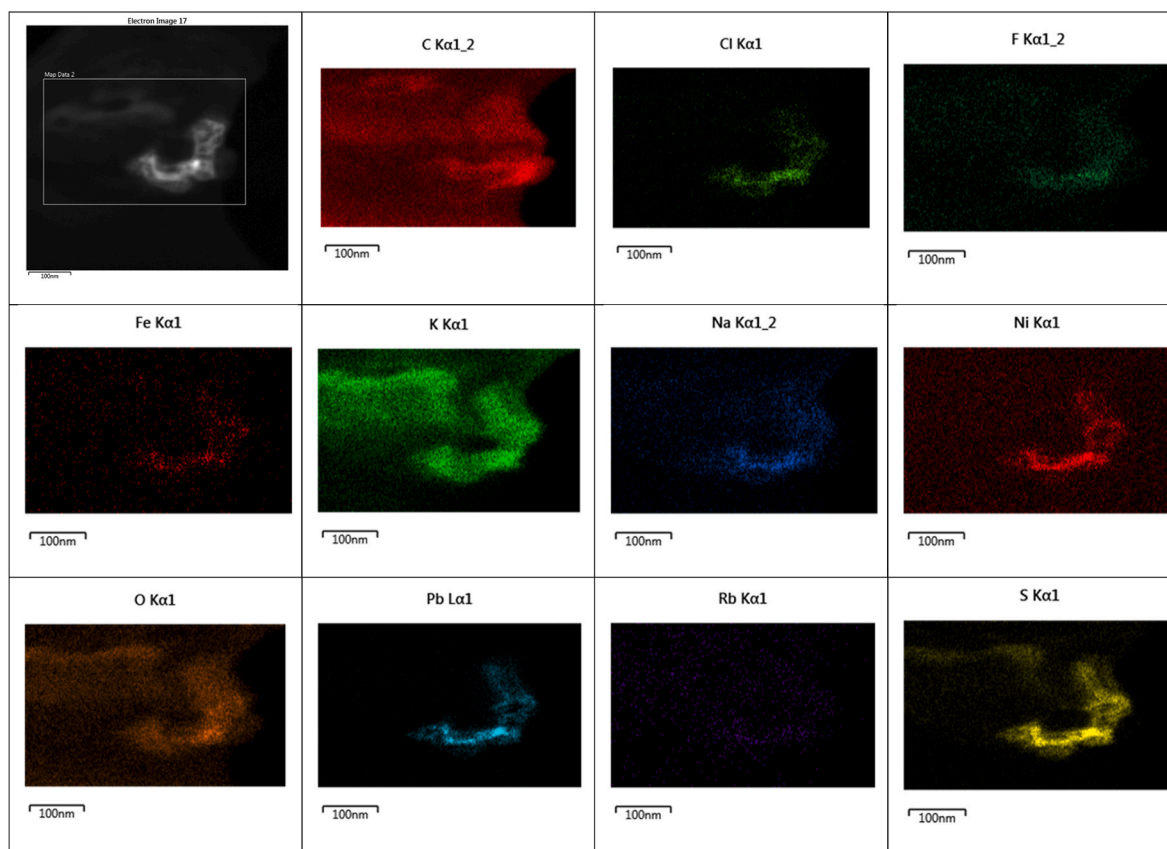
Fig. 7. Dark field image and elemental map of particle found in Office 1.

3.2. Relative elemental contribution to spectra of individual particles

Table 2 summarises the relative contribution of each element to the particles characterised in each of the five indoor microenvironments. Si and Fe are the most prevalent elements observed in particles with size <250 nm, with elemental contributions to individual particles ranging from 13 to 39% (Si) and 3%–34% (Fe). The third most abundant element found is S, with elemental contributions ranging 9%–19%. Si, Fe and S were found in particles collected in the five microenvironments. Si can originate from mineral matter in soil and dust (Viana et al., 2008) and can be a constituent of paper (Lourenco et al., 2015), especially relevant in office environments. Fe can be related to the brake wear and vehicle exhaust (Viana et al., 2008) and can originate also from soil and dust (Harrison and Yin, 2010). S is typically associated with fuel combustion (Khodeir et al., 2012), industry emissions and secondary aerosols (Viana et al., 2008). The elements from outdoor origin can infiltrate through the building envelope (Vu et al., 2017b) or access indoor environments through open windows (Hussein and Kulmala, 2008). In addition, constituents of soil and dust can be introduced indoors by humans (Thatcher and Layton, 1995), for instance attached to shoes and clothes, and can be later re-suspended by human (or pet) movements.

Less abundant elements are K (0.4%–16%), Na (2.5%–12%) and Cr (0.5–5.4%), found in 80% of indoor samples; and Ca (3.1%–42%) and Cl (0.9%–6.4%), found in 60% of studied microenvironments. K, Na, and Ca can be from mineral soil origin. Cr is likely associated with stainless steel utensils used indoors (Li et al., 2015), or with industrial emissions (Khodeir et al., 2012) from outdoor origin penetrating indoors.

Other metal species (Table 2) were found only in 1 or 2 indoor locations, with elemental contributions ranging from 0.08% (Co) to 5.6% (Cu). Possible origins of these minor metal constituents could be related to mineral soil and dust, vehicular emissions, marine spray, stainless steel utensils, printer inks, paper, secondary aerosols, solid fuel combustion, electronic constituents and flame-retardants as summarised in Table 3.

In the present study some elements e.g. Be, could not be linked directly to any indoor sources/activities or with sources relevant to outdoor air emitting particles that could have penetrated indoors. A study conducted in residences in several U.S. cities also reported that a substantial portion of indoor particles could not be linked with any known sources (Wallace, 1996).

3.3. Particle size distribution of particles measured in each site

Table 1 (Figure S1) shows the aerodynamic particle sizes collected on the Ni grid mounted on the <250 nm size fraction of the impactor for each of the indoor locations measured. The number of particles counted per site were Home 1–338, Home 2–24, Home 3–188, Office 1–75 and Office 3–49. Across the 5 sites, the average particle sizes range from 35 ± 59 nm 103 ± 160 nm, which is consistent with the nominal size fraction collected by this impactor stage (<250 nm). However, inspection of the histograms of particles collected on the grids (Figure S1) shows that the sizes of some of the particles were larger. This could be because of particle bounce or re-entrainment of particles from a higher stage of the impactor to a lower stage. It could also be the result of the single particles or primary particles (PP) or loosely attached particle (agglomerates) coming in contact with each other during collection, thus becoming tightly attached by metallic, ionic or covalent bonds resulting in the formation of aggregates. Some of these aggregates appear as a single particle with a diameter as large as 1000 nm, despite being collected on a <250 nm size fraction of the impactor (e.g., see Fig. 8). This could be due to particle bounce during sampling. Studies have shown that due to the physical principle of particle collection associated with all impactors, sampling artefacts like particle bounce from a larger size cut-off above into the next stage can occur (Fonseca
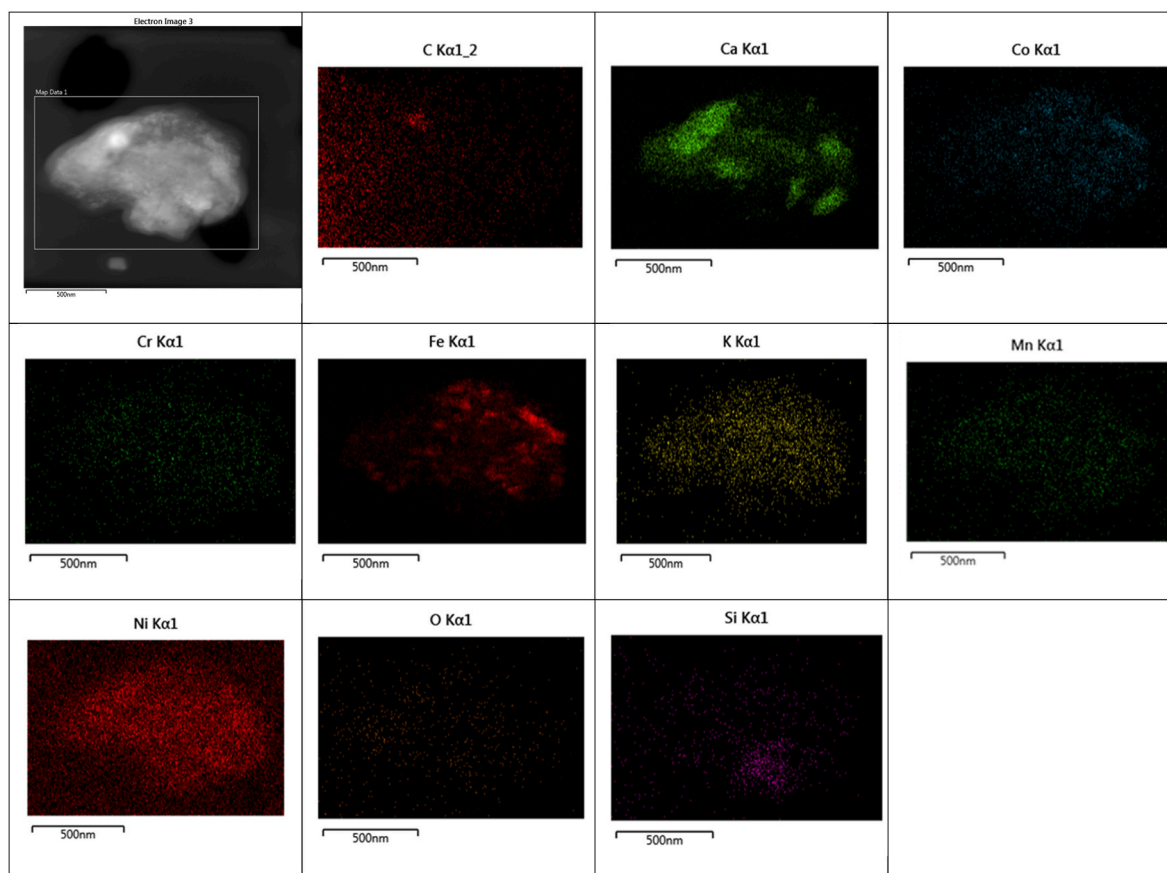
Fig. 8. Dark field image and elemental map of particle found in Office 2 (Map room and Photocopying/printing room).

et al., 2016; Wall et al., 1988). Fonseca et al. (2016) suggests that particle bounce can be expected when using the cascade impactor during dry collect or indoors as in the case of this study.

The frequency of particle sizes observed during the TEM analysis is shown in Figure S1. The smallest mean was observed in Office 1, which was sampled in the summer and the office window was opened. The opened window faced a car park that parks 12 cars and a minor road (inside the university). The small sizes observed may be due to vehicle-related pollution penetrating into the office from the open window. Home 1 had the highest amount of particles counted on the grid not only because it sampled for the longest amount of time but because various indoor activities were conducted that are known sources of ultrafine particles (Vu et al., 2017a) e.g. cooking, sweeping and other house chores were in progress during collection of the sample. This cooking activity also accounts for the small mean size of the particles collected. This is similar to what other researchers have observed (Abdullahi et al., 2013). One study observed mode diameters of 40 nm, 50 nm, and 30 nm during scrambling eggs, frying chicken and cooking soups respectively (Li et al., 1993). Another study showed that cooking processes produced peak numbers of particles between 22 and 72 nm (Dennekamp et al., 2001). Generation of particles in Home 1 and Home 2 resulted from cooking activities, cleaning and movement of people, whereas in Home 3 the only indoor activity observed was people movement, so most probably the movement of people caused the resuspension of indoor particles that were collected with the impactor. These activities have been suggested to have significant impact on indoor particle concentrations (Abt et al., 2000; Wallace et al., 2013). Home 2 and Office 2 appeared to have a bimodal distribution but the primary mode was in the <100 nm size range, whereas Home 1, Home 3 and Office 1 showed a single mode with prevalent particle size also in the size range <100 nm (Figure S1).

3.4. Implications of the size, shape and surface chemistry of the indoor particles

Understanding indoor particles and exposure to them is important in order to help identify how these particles may affect humans and to facilitate the implementation of possible control measures to reduce emissions indoor. This is especially relevant for particles in the ultrafine range because their physicochemical properties can be different from those in the bulk size range (Buzea et al., 2007; Stone et al., 2007). A range of particles were collected indoors (home and offices) in the current study, showing different particle sizes in the ultrafine region and shapes with a wide range of chemical compositions (Figs. 1–8). Size is one of the most important characteristics defining the pattern of regional deposition in the respiratory tract (Ou et al., 2020). Of the particles viewed under the TEM, those with <100 nm appeared to have the highest frequency (Table 1). Whilst particles larger than 1 μm are deposited preferentially in the extra-thoracic area, particles smaller than 1 μm are deposited throughout the entire respiratory tract and have the ability to reach the bronchi and alveoli (Geiser and Kreyling, 2010). The lung burden (determined by the concentration and rate of deposition and clearance) of these particles depends on the size, shape and chemical characteristics of the particle. Smaller particles as observed in this study may have higher toxicity in comparison to larger particles because of their large surface area (Brown et al., 2001), thus possibly higher chemical bioavailability and potential to react with the lung lining fluid and access respiratory epithelium cells. They may also have longer residence time in the lungs since smaller particles can more easily evade the clearance system and phagocytosis. Smaller particles also have the potential to translocate to the blood stream through a variety of cellular mechanisms such as endocytosis (Muhlfeld et al., 2008), diffusion or adhesive interactions (Geiser et al., 2005). Smaller particles in the

Table 3
Summary of list of elements observed in primary particles and agglomerates, their location and possible sources.

Elements	Possible sources	Location and activity description					References
		Home 1	Home 2	Home 3	Office 1	Office 2	
		Indoor house chores (cleaning and sweeping) and cooking	Indoor house chores (cleaning and sweeping)	No indoor activities, except for dweller's movement	Window open opposite a car park	Map room, photocopying and printing	
Si, Fe	Mineral contents from soil	X	X	X	X	X	Viana et al. (2008)
Al			X				
Ca		X	X			X	
K		X	X	X		X	
S	Fuel combustion	X	X	X	X	X	Khodeir et al. (2012)
	Industry emissions						Viana et al. (2008)
	Secondary aerosols						Viana et al. (2008)
Ni	Stainless steel: from	X					Li et al. (2015)
Cr	cooking utensil and coating	X	X	X		X	
Fe	of finishes in the house	X	X	X	X	X	
Ti		X					
Cu		X	X				
Mo		X					
Sn	Tin cans (food storage)	X					(RSC)
	Tin salts coating electrically conductive glass						Zhang et al. (2006)
	Fire-retardant used in plastics						Horrocks et al. (2010)
Na	Marine origin i.e. water		X	X	X	X	Viana et al. (2008)
Cl	body spray		X		X	X	
P	Coke or wood burning (e.g. for domestic or commercial heating)		X				Pernigotti et al. (2016)
	Use in fertilizers Power plant emissions						
F	Secondary aerosol				X		Karar and Gupta (2007)
	Coal combustion				X		Zhang and Smith (2007)
Pb, Rb	Road dust emissions				X		Pant and Harrison (2013)
Ni, Fe, Si, Mn	Printer toner and inks					X	Martin et al. (2015)
Co							Brown et al. (2018)
Ca	Paper					X	Martin et al. (2015)

nanosize range have also been observed to translocate through the olfactory bulb (Wang et al., 2008; Yu et al., 2007), potentially becoming a route of entry to the brain (Oberdorster et al., 2004), and nanoparticles have been observed in the brain (Li et al., 2016; Maher et al., 2016).

Particles observed in this study exist typically as aggregates rather than as single particles, and thus some of these aggregates have sizes greater than 100 nm. When these aggregates are inhaled, they can be more easily removed by the alveolar macrophage through phagocytosis than nanosized particles. However, the shape of the particles defines their clearance (Zhao et al., 2019) as well as their toxicity (Warheit et al., 2006). In this study, different shapes of particles were observed, such as irregular shape, spherical, non-spherical, rods, fibre, hexagonal, and aggregate (Figs. 1–8). Non-spherical particles have a higher surface area than the spherical particles of comparable aerodynamic diameter, thereby providing potentially more surface contact for interaction with the lungs (Carabali et al., 2012). Bound to these particles are trace metals, organic species and other compounds. For example, insoluble compounds may be able to cause inflammation and oxidative stress by direct particle reaction with the airways as compared to soluble compounds that are dissolved and can pass into the circulatory system (Karlsson et al., 2005; Knaapen et al., 2002). Some of these chemical components may have the ability to trigger inflammation, oxidative stress and other negative health effects (Kelly and Fussell, 2012).

3.5. Strengths and limitations

This study has characterised the morphology, size and surface chemistry of quasi-ultrafine particles collected from indoor environments, such as homes and offices. The results provided add evidence of the physicochemical properties of indoor quasi-ultrafine particles, which is a field with scarcity of data. The evidence generated can help in understanding the hazard and fate of qUFP in the human body.

On the other hand, this study presents also some limitations. First, samples of qUFP were collected only in five indoor environments. Nonetheless, sufficient number of qUFP were collected allowing to provide an overview of a range of morphologies, sizes and chemistries of qUFP encountered in indoor environments. Another limitation was that the sampling methodology had to be adjusted during the initial samples, as filters were overloaded, or not sufficiently loaded, until the optimum sampling time was determined. It is recommended to sample for 2 h to collect sufficient material on the TEM grids for physico-chemical characterisation of indoor qUFP. Despite the differential sampling times, the filters had provided novel data on the physicochemical characteristics of qUFP, and thus the insights extracted from those initial two filters have been analysed and discussed. A technical limitation during particle imaging was the fact that it was difficult to switch between bright and dark imaging to capture the same particles to obtained both sharp

images of them alongside their chemical characterisation. For these reason, the dark field images of the particles taken alongside the chemical characterisation are less focused as those that would have been obtained using bright field images. Despite that, valuable information could be obtained on the morphology and size of those particles with chemical characterization. Finally, the discussion of the of source identifications of those particles relies on detection of specific elements, or clusters of elements identified from the target particles, but does not use the chemical profile of possible sources, as currently, it does not exist for many of the indoor sources. Therefore, the sources proposed in this work are considered to be suggestions based on the specific elements identified in the particles that are known to be present in the suggested sources. However, these particles might originate from other possible sources not identified in the current study. Further studies should characterise the physicochemical profile of typical indoor sources, such as cooking, printing (e.g. emissions from the use of paper, toner and ink), cleaning, incense burning, and use of personal care products, among others. Once these physicochemical profiles become available, further studies would be able to provide new evidence to ascertain the likelihood of the sources identified in the current study.

4. Conclusion

A variety of quasi-ultrafine particles (<250 nm) from several indoor environments have been collected using a cascade impactor and characterised by electron microscopy (TEM/EDS). The size of these particles is predominantly below 100 nm; their shape is mainly irregular, with some instances of rod-like particles; and their chemical components are primarily Fe, Si and S. The physico-chemical properties of these particles determine their toxicological fate by defining the depth of inhalation, deposition and lung burden, their clearance rate and ability to translocate to the blood stream, as well as their toxicity associated with adsorbed, absorbed or core constituents of these nanosized indoor air particles.

Despite the limited number of indoor environments surveyed and low replication of samples collected and characterised, this study has combined two robust methodologies to characterise indoor air quasi-ultrafine particles. Thus, the current study provides information on physicochemical properties of a number of particles collected in indoor environments, such as size, shape and composition, and helps filling a gap of knowledge. Further studies characterising the physicochemical properties of a larger number of particles in a wider variety of indoor environments, as well as from different geographical areas is highly recommended.

CRediT authorship contribution statement

Adobi Okam: Data curation, Formal analysis, Investigation, Visualization, Writing – original draft, Writing – review & editing. **Paul Sanderson:** Data curation, Investigation, Visualization, Writing – review & editing. **Roy M. Harrison:** Conceptualization, Methodology, Project administration, Resources, Supervision, Writing – review & editing. **Juana Maria Delgado-Saborit:** Conceptualization, Data curation, Methodology, Project administration, Resources, Supervision, Validation, Visualization, Writing – original draft, Writing – review & editing.

Declaration of competing interest

The authors declare that they have no known competing financial interests or personal relationships that could have appeared to influence the work reported in this paper.

Data availability

Data will be made available on request.

Appendix A. Supplementary data

Supplementary data to this article can be found online at https://doi.org/10.1016/j.atmosenv.2023.120245.

References

Abdullahi, K.L., Delgado-Saborit, J.M., Harrison, R.M., 2013. Emissions and indoor concentrations of particulate matter and its specific chemical components from cooking: a review. Atmos. Environ. 71, 260–294.

Abt, E., Suh, H.H., Allen, G., Koutrakis, P., 2000. Characterization of indoor particle sources: a study conducted in the metropolitan Boston area. Environ. Health Perspect. 108, 35.

Adachi, K., Buseck, P., 2008. Internally mixed soot, sulfates, and organic matter in aerosol particles from Mexico City. Atmos. Chem. Phys. 8, 6469–6481.

Albanese, A., Tang, P.S., Chan, W.C., 2012. The effect of nanoparticle size, shape, and surface chemistry on biological systems. Annu. Rev. Biomed. Eng. 14, 1–16.

Ali, M.U., Lin, S.Y.Y., Yousaf, B., Abbas, Q., Munir, M.A.M., Rashid, A., Zheng, C.M., Kuang, X.X., Wong, M.H., 2022. Pollution characteristics, mechanism of toxicity and health effects of the ultrafine particles in the indoor environment: current status and future perspectives. Crit. Rev. Environ. Sci. Technol. 52, 436–473.

Araujo, J.A., Barajas, B., Kleinman, M., Wang, X.P., Bennett, B.J., Gong, K.W., Navab, M., Harkema, J., Sioutas, C., Lusis, A.J., Nel, A.E., 2008. Ambient particulate pollutants in the ultrafine range promote early atherosclerosis and systemic oxidative stress. Circ. Res. 102, 589–596.

Arora, P., Jain, S., 2015. Morphological characteristics of particles emitted from combustion of different fuels in improved and traditional cookstoves. J. Aerosol Sci. 82, 13–23.

Auffan, M., Rose, J., Bottero, J.-Y., Lowry, G.V., Jolivet, J.-P., Wiesner, M.R., 2009. Towards a definition of inorganic nanoparticles from an environmental, health and safety perspective. Nat Nano 4, 634–641.

Brouwer, D.H., Gijsbers, J.H.J., Lurvink, M.W.M., 2004. Personal exposure to ultrafine particles in the workplace: exploring sampling techniques and strategies. Ann. Occup. Hyg. 48, 439–453.

Brown, D.M., Wilson, M.R., MacNee, W., Stone, V., Donaldson, K., 2001. Size-dependent proinflammatory effects of ultrafine polystyrene particles: a role for surface area and oxidative stress in the enhanced activity of ultrafines. Toxicol. Appl. Pharmacol. 175, 191–199.

Brown, D.M., Johnston, H.J., Gaiser, B., Pinna, N., Caputo, G., Culha, M., Kelestemur, S., Altunbek, M., Stone, V., Roy, J.C., Kinross, J.H., Fernandes, T.F., 2018. A cross-species and model comparison of the acute toxicity of nanoparticles used in the pigment and ink industries. Nanoimpact 11, 20–32.

Buzea, C., Pacheco II, Robbie, K., 2007. Nanomaterials and nanoparticles: sources and toxicity. Biointerphases 2, MR17–MR71.

Campagnolo, L., Massimiani, M., Magrini, A., Camaioni, A., Pietroiusti, A., 2012. Physico-chemical properties mediating reproductive and developmental toxicity of engineered nanomaterials. Curr. Med. Chem. 19, 4488–4494.

Carabali, G., Mamani-Paco, R., Castro, T., Peralta, O., Herrera, E., Trujillo, B., 2012. Optical properties, morphology and elemental composition of atmospheric particles at T1 supersite on MILAGRO campaign. Atmos. Chem. Phys. 12, 2747–2755.

Chithra, V., Nagendra, S.S., 2013. Chemical and morphological characteristics of indoor and outdoor particulate matter in an urban environment. Atmos. Environ. 77, 579–587.

Delgado-Saborit, J.M., 2019. Indoor air as a contributor to air pollution exposure. In: Harrison, R.M., Hester, R.E. (Eds.), Indoor Air Pollution. Royal Soc Chemistry, Cambridge, pp. 158–195.

Delgado-Saborit, J.M., Aquilina, N.J., Meddings, C., Baker, S., Harrison, R.M., 2011. Relationship of personal exposure to volatile organic compounds to home, work and fixed site outdoor concentrations. Sci. Total Environ. 409, 478–488.

Dennekamp, M., Howarth, S., Dick, C., Cherrie, J., Donaldson, K., Seaton, A., 2001. Ultrafine particles and nitrogen oxides generated by gas and electric cooking. Occup. Environ. Med. 58, 511–516.

Diapouli, E., Chaloulakou, A., Koutrakis, P., 2013. Estimating the concentration of indoor particles of outdoor origin: a review. J. Air Waste Manag. Assoc. 63, 1113–1129.

Donaldson, K., Stone, V., Seaton, A., MacNee, W., 2001. Ambient particle inhalation and the cardiovascular system: potential mechanisms. Environ. Health Perspect. 109, 523–527.

Fonseca, A.S., Talbot, N., Schwarz, J., Ondráček, J., Ždímal, V., Kozáková, J., Viana, M., Karanasiou, A., Querol, X., Alastuey, A., Vu, T.V., Delgado-Saborit, J.M., Harrison, R. M., 2016. Intercomparison of four different cascade impactors for fine and ultrafine particle sampling in two European locations. Atmos. Chem. Phys. Discuss. 1–27, 2016.

Fromme, H., 2012. Particles in the Indoor Environment. INTECH Open Access Publisher.

Gatoo, M.A., Naseem, S., Arfat, M.Y., Mahmood Dar, A., Qasim, K., Zubair, S., 2014. Physicochemical properties of nanomaterials: implication in associated toxic manifestations. BioMed Res. Int. 2014, 498420.

Geiser, M., Kreyling, W.G., 2010. Deposition and biokinetics of inhaled nanoparticles. Part. Fibre Toxicol. 7, 2.

Geiser, M., Rothen-Rutishauser, B., Kapp, N., Schurch, S., Kreyling, W., Schulz, H., Semmler, M., Hof, V.I., Heyder, J., Gehr, P., 2005. Ultrafine particles cross cellular membranes by nonphagocytic mechanisms in lungs and in cultured cells. Environ. Health Perspect. 113, 1555–1560.

Geng, H., Kang, S., Jung, H.-J., Choël, M., Kim, H., Ro, C.-U., 2010. Characterization of individual submicrometer aerosol particles collected in Incheon, Korea, by quantitative transmission electron microscopy energy-dispersive X-ray spectrometry. J. Geophys. Res. Atmos. 115 n/a-n/a.

Gerber, N., Scheeder, M.R., Wenk, C., 2009. The influence of cooking and fat trimming on the actual nutrient intake from meat. Meat Sci. 81, 148–154.

Glytsos, T., Ondráček, J., Dzumbová, L., Kopanakis, I., Lazaridis, M., 2010. Characterization of particulate matter concentrations during controlled indoor activities. Atmos. Environ. 44, 1539–1549.

Hammer, S.E., Ervik, T., Ellingsen, D.G., Thomassen, Y., Weinbruch, S., Benker, N., Berlinger, B., 2021. Particle characterisation and bioaccessibility of manganese in particulate matter in silico- and ferromanganese smelters. Environ. Sci. Proc. Impact. 23, 1488–1499.

Handy, R., von der Kammer, F., Lead, J., Hassellöv, M., Owen, R., Crane, M., 2008. The ecotoxicology and chemistry of manufactured nanoparticles. Ecotoxicology 17, 287–314.

Hankin, J.H., Margen, S., Goldsmith, N.F., 1970. Contribution of hard water to calcium and magnesium intakes of adults. J. Am. Diet Assoc. 56, 212–224.

Hänninen, O., Lebret, E., Ilacqua, V., Katsouyanni, K., Künzli, N., Srám, R.J., Jantunen, M., 2004. Infiltration of ambient PM 2.5 and levels of indoor generated non-ETS PM 2.5 in residences of four European cities. Atmos. Environ. 38, 6411–6423.

Harrison, R.M., Yin, J.X., 2010. Chemical speciation of PM2.5 particles at urban background and rural sites in the UK atmosphere. J. Environ. Monit. 12, 1404–1414.

Heusinkveld, H.J., Wahle, T., Campbell, A., Westerink, R.H.S., Tran, L., Johnston, H., Stone, V., Cassee, F.R., Schins, R.P.F., 2016. Neurodegenerative and neurological disorders by small inhaled particles. Neurotoxicology 56, 94–106.

Höppe, P., Martinac, I., 1998. Indoor climate and air quality. Int. J. Biometeorol. 42, 1–7.

Horrocks, A.R., Smart, G., Nazare, S., Kandola, B., Price, D., 2010. Quantification of zinc hydroxystannate** and stannate** synergies in halogen-containing flame-retardant polymeric formulations. J. Fire Sci. 28, 217–248.

Hou, C.C., Zhu, J.Q., 2017. Nanoparticles and female reproductive system: how do nanoparticles affect oogenesis and embryonic development. Oncotarget 8, 109799–109817.

Hu, D., Alfarra, M.R., Szpek, K., Langridge, J.M., Cotterell, M.I., Belcher, C., Rule, I., Liu, Z., Yu, C., Shao, Y., Voliotis, A., Du, M., Smith, B., Smallwood, G., Lobo, P., Liu, D., Haywood, J.M., Coe, H., Allan, J.D., 2021. Physical and chemical properties of black carbon and organic matter from different combustion and photochemical sources using aerodynamic aerosol classification. Atmos. Chem. Phys. 21, 16161–16182.

Hussein, T., Kulmala, M., 2008. Indoor aerosol modeling: basic principles and practical applications. Water Air Soil Pollut. Focus 8, 23–34.

Kang, S., Hwang, H., Kang, S., Park, Y., Kim, H., Ro, C.-U., 2009. Quantitative ED-EPMA combined with morphological information for the characterization of individual aerosol particles collected in Incheon, Korea. Atmos. Environ. 43, 3445–3453.

Karar, K., Gupta, A.K., 2007. Source apportionment of PM10 at residential and industrial sites of an urban region of Kolkata, India. Atmos. Res. 84, 30–41.

Karlsson, H.L., Nilsson, L., Möller, L., 2005. Subway particles are more genotoxic than street particles and induce oxidative stress in cultured human lung cells. Chem. Res. Toxicol. 18, 19–23.

Kelly, F.J., Fussell, J.C., 2012. Size, source and chemical composition as determinants of toxicity attributable to ambient particulate matter. Atmos. Environ. 60, 504–526.

Khatri, M., Bello, D., Gaines, P., Martin, J., Pal, A.K., Gore, R., Woskie, S., 2013. Nanoparticles from photocopiers induce oxidative stress and upper respiratory tract inflammation in healthy volunteers. Nanotoxicology 7, 1014–1027.

Khodeir, M., Shamy, M., Alghamdi, M., Zhong, M., Sun, H., Costa, M., Chen, L.-C., Maciejczyk, P., 2012. Source apportionment and elemental composition of PM2.5 and PM10 in Jeddah city, Saudi arabia. Atmos. Pollut. Res. 3, 331–340.

Kimura, M., Itokawa, Y., 1990. Cooking losses of minerals in foods and its nutritional significance. J. Nutr. Sci. Vitaminol. 36 (Suppl 1), S25–S32 discussion S33.

Knaapen, A.M., Shi, T., Borm, P.J., Schins, R.P., 2002. Soluble Metals as Well as the Insoluble Particle Fraction Are Involved in Cellular DNA Damage Induced by Particulate Matter, Oxygen/Nitrogen Radicals: Cell Injury and Disease. Springer, pp. 317–326.

Lazaridis, M., 2011. Indoor Air Pollution First Principles of Meteorology and Air Pollution. Springer Netherlands, pp. 255–304.

Li, C.-S., Lin, W.-H., Jenq, F.-T., 1993. Size distributions of submicrometer aerosols from cooking. Environ. Int. 19, 147–154.

Li, N., Sioutas, C., Cho, A., Schmitz, D., Misra, C., Sempf, J., Wang, M., Oberley, T., Froines, J., Nel, A., 2003. Ultrafine particulate pollutants induce oxidative stress and mitochondrial damage. Environ. Health Perspect. 111, 455–460.

Li, Y.-C., Shu, M., Ho, S.S.H., Wang, C., Cao, J.-J., Wang, G.-H., Wang, X.-X., Wang, K., Zhao, X.-Q., 2015. Characteristics of PM2.5 emitted from different cooking activities in China. Atmos. Res. 166, 83–91.

Li, D.S., Morishita, M., Wagner, J.G., Fatouraie, M., Wooldridge, M., Eagle, W.E., Barres, J., Carlander, U., Emond, C., Jolliet, O., 2016. In vivo biodistribution and physiologically based pharmacokinetic modeling of inhaled fresh and aged cerium oxide nanoparticles in rats. Part. Fibre Toxicol. 13, 20.

Li, Y., Wu, A., Wu, Y., Xu, J., Zhao, Z., Tong, M., Shengji, L., 2019. Morphological characterization and chemical composition of PM2.5 and PM10 collected from four typical Chinese restaurants. Aerosol. Sci. Technol. 53, 1186–1196.

Long, C.M., Suh, H.H., Kobzik, L., Catalano, P.J., Ning, Y.Y., Koutrakis, P., 2001. A pilot investigation of the relative toxicity of indoor and outdoor fine particles: in vitro effects of endotoxin and other particulate properties. Environ. Health Perspect. 109, 1019.

Lourenco, A.F., Gamelas, J.A.F., Sequeira, J., Ferreira, P.J., Velho, J.L., 2015. Improving paper mechanical properties using silica-modified ground calcium carbonate as filler. Bioresources 10, 8312–8324.

Maher, B.A., Ahmed, I.A.M., Karloukovski, V., MacLaren, D.A., Foulds, P.G., Allsop, D., Mann, D.M.A., Torres-Jardón, R., Calderon-Garciduenas, L., 2016. Magnetite pollution nanoparticles in the human brain. Proc. Natl. Acad. Sci. USA 113, 10797–10801.

Manigrasso, M., Protano, C., Vitali, M., Avino, P., 2019. Where do ultrafine particles and nano-sized particles come from? J. Alzheim. Dis. 68, 1371–1390.

Martin, J., Bello, D., Bunker, K., Shafer, M., Christiani, D., Woskie, S., Demokritou, P., 2015. Occupational exposure to nanoparticles at commercial photocopy centers. J. Hazard Mater. 298, 351–360.

Marval, J., Tronville, P., 2022. Ultrafine particles: a review about their health effects, presence, generation, and measurement in indoor environment. Build. Environ. 216.

Maskey, S., Kim, J.-S., Cho, H.-J., Park, K., 2012. Ultrafine particle events in the ambient atmosphere in Korea. Asian J. Atmos. Environ. 6, 288–303.

Morawska, L., Ayoko, G.A., Bae, G.N., Buonanno, G., Chao, C.Y.H., Clifford, S., Fu, S.C., Hänninen, O., He, C., Isaxon, C., Mazaheri, M., Salthammer, T., Waring, M.S., Wierzbicka, A., 2017. Airborne particles in indoor environment of homes, schools, offices and aged care facilities: the main routes of exposure. Environ. Int. 108, 75–83.

Muhlfeld, C., Gehr, P., Rothen-Rutishauser, B., 2008. Translocation and cellular entering mechanisms of nanoparticles in the respiratory tract. Swiss Med. Wkly. 138, 387–391.

Oberdorster, G., Sharp, Z., Atudorei, V., Elder, A., Gelein, R., Kreyling, W., Cox, C., 2004. Translocation of inhaled ultrafine particles to the brain. Inhal. Toxicol. 16, 437–445.

Oberdörster, G., Maynard, A., Donaldson, K., Castranova, V., Fitzpatrick, J., Ausman, K., Carter, J., Karn, B., Kreyling, W., Lai, D., Olin, S., Monteiro-Riviere, N., Warheit, D., Yang, H., 2005a. Principles for characterizing the potential human health effects from exposure to nanomaterials: Elements of a screening strategy. Part Fibre Toxicol. 2, 8.

Oberdörster, G., Oberdörster, E., Oberdörster, J., 2005b. Nanotoxicology: an emerging discipline evolving from studies of ultrafine particles. Environ. Health Perspect. 113, 823–839.

Ogulei, D., Hopke, P., Wallace, L., 2006. Analysis of indoor particle size distributions in an occupied townhouse using positive matrix factorization. Indoor Air 16, 204–215.

Okam, A.U., 2017. Personal and Indoor Exposure to Nanoparticles and its Relationship to Biological Markers. University of Birmingham.

Ott, E.-J.E., Kucinski, T.M., Dawson, J.N., Freedman, M.A., 2021. Use of transmission electron microscopy for analysis of aerosol particles and strategies for imaging fragile particles. Anal. Chem. 93, 11347–11356.

Ou, C., Hang, J., Deng, Q., 2020. Particle deposition in human lung airways: effects of airflow, particle size, and mechanisms. Aerosol Air Qual. Res. 20, 2846–2858.

Pant, P., Harrison, R.M., 2013. Estimation of the contribution of road traffic emissions to particulate matter concentrations from field measurements: a review. Atmos. Environ. 77, 78–97.

Pernigotti, D., Belis, C.A., Spanò, L., 2016. SPECIEUROPE: the European data base for PM source profiles. Atmos. Pollut. Res. 7, 307–314.

Pipal, A.S., Rohra, H., Tiwari, R., Taneja, A., 2021. Particle size distribution, morphometric study and mixing structure of accumulation and ultrafine aerosols emitted from indoor activities in different socioeconomic micro-environment. Atmos. Pollut. Res. 12, 101–111.

Pope, C.A. 3rd, 2000. Epidemiology of fine particulate air pollution and human health: biologic mechanisms and who's at risk? Environ. Health Perspect. 108, 713–723.

Pope, C.A. 3rd, Dockery, D.W., 2006. Health effects of fine particulate air pollution: lines that connect. J. Air Waste Manag. Assoc. 56, 709–742.

Renwick, L.C., Brown, D., Clouter, A., Donaldson, K., 2004. Increased inflammation and altered macrophage chemotactic responses caused by two ultrafine particle types. Occup. Environ. Med. 61, 442–447.

Rosen, H.N., Salemme, H., Zeind, A.J., Moses, A.C., Shapiro, A., Greenspan, S.L., 1994. Chicken soup revisited: calcium content of soup increases with duration of cooking. Calcif. Tissue Int. 54, 486–488.

RSC Periodic Table: Tin. In: Chemistry, R. S. O. (ed.).

Sanderson, P., 2015. Measurement and Identification of Ambient Atmospheric Metallic Nanoparticles, School of Geography, Earth and Environmental Sciences. University of Birmingham, p. 336.

Sanderson, P., Su, S.S., Chang, I.T.H., Saborit, J.M.D., Kepaptsoglou, D.M., Weber, R.J. M., Harrison, R.M., 2016. Characterisation of iron-rich atmospheric submicrometre particles in the roadside environment. Atmos. Environ. 140, 167–175.

Sengupta, P., 2013. Potential health impacts of hard water. Int. J. Prev. Med. 4, 866–875.

Shehab, M., Pope, F.D., Delgado-Saborit, J.M., 2021. The contribution of cooking appliances and residential traffic proximity to aerosol personal exposure. J. Environ. Health Sci. Eng. 19, 307–318.

Stewart, J.C., Chalupa, D.C., Devlin, R.B., Frasier, L.M., Huang, L.S., Little, E.L., Lee, S. M., Phipps, R.P., Pietropaoli, A.P., Taubman, M.B., Utell, M.J., Frampton, M.W., 2010. Vascular effects of ultrafine particles in persons with type 2 diabetes. Environ. Health Perspect. 118, 1692–1698.

Stoehr, L.C., Gonzalez, E., Stampfl, A., Casals, E., Duschl, A., Puntes, V., Oostingh, G.J., 2011. Shape matters: effects of silver nanospheres and wires on human alveolar epithelial cells. Part. Fibre Toxicol. 8, 36.

Stone, V., Johnston, H., Clift, M.J.D., 2007. Air pollution, ultrafine and nanoparticle toxicology: cellular and molecular interactions. IEEE Trans. NanoBioscience 6, 331–340.

Stone, V., Nowack, B., Baun, A., van den Brink, N., von der Kammer, F., Dusinska, M., Handy, R., Hankin, S., Hassellöv, M., Joner, E., Fernandes, T.F., 2010. Nanomaterials for environmental studies: classification, reference material issues, and strategies for physico-chemical characterisation. Sci. Total Environ. 408, 1745–1754.

Szymczak, W., Menzel, N., Keck, L., 2007. Emission of ultrafine copper particles by universal motors controlled by phase angle modulation. J. Aerosol Sci. 38, 520–531.

Taner, S., Pekey, B., Pekey, H., 2013. Fine particulate matter in the indoor air of barbeque restaurants: elemental compositions, sources and health risks. Sci. Total Environ. 454, 79–87.

Thatcher, T.L., Layton, D.W., 1995. Deposition, resuspension, and penetration of particles within a residence. Atmos. Environ. 29, 1487–1497.

Toyokuni, S., 1999. Reactive oxygen species-induced molecular damage and its application in pathology. Pathol. Int. 49, 91–102.

Vardoulakis, S., Giagloglou, E., Steinle, S., Davis, A., Sleeuwenhoek, A., Galea, K.S., Dixon, K., Crawford, J.O., 2020. Indoor exposure to selected air pollutants in the home environment: a systematic review. Int. J. Environ. Res. Publ. Health 17.

Viana, M., Kuhlbusch, T.A.J., Querol, X., Alastuey, A., Harrison, R.M., Hopke, P.K., Winiwarter, W., Vallius, M., Szidat, S., Prévôt, A.S.H., Hueglin, C., Bloemen, H., Wåhlin, P., Vecchi, R., Miranda, A.I., Kasper-Giebl, A., Maenhaut, W., Hitzenberger, R., 2008. Source apportionment of particulate matter in Europe: a review of methods and results. J. Aerosol Sci. 39, 827–849.

Vinzents, P.S., Møller, P., Sørensen, M., Knudsen, L.E., Hertel, O., Jensen, F.P., Schibye, B., Loft, S., 2005. Personal exposure to ultrafine particles and oxidative DNA damage. Environ. Health Perspect. 113, 1485.

Vu, T.V., Ondracek, J., Zdimal, V., Schwarz, J., Delgado-Saborit, J.M., Harrison, R.M., 2017a. Physical properties and lung deposition of particles emitted from five major indoor sources. Air Qual. Atmos. Health 10, 1–14.

Vu, T.V., Zauli-Sajani, S., Poluzzi, V., Delgado-Saborit, J.M., Harrison, R.M., 2017b. Loss processes affecting submicrometer particles in a house heavily affected by road traffic emissions. Aerosol. Sci. Technol. 51, 1201–1211.

Wall, S.M., John, W., Ondo, J.L., 1988. Measurement of aerosol size distributions for nitrate and major ionic species. Atmos. Environ. 22, 1649–1656, 1967.

Wallace, L., 1996. Indoor particles: a review. J. Air Waste Manag. Assoc. 46, 98–126.

Wallace, L., Ott, W., 2011. Personal exposure to ultrafine particles. J. Expo. Sci. Environ. Epidemiol. 21, 20–30.

Wallace, L., Kindzierski, W., Kearney, J., MacNeill, M., Héroux, M.-È., Wheeler, A.J., 2013. Fine and ultrafine particle decay rates in multiple homes. Environ. Sci. Technol. 47, 12929–12937.

Wang, J.X., Liu, Y., Jiao, F., Lao, F., Li, W., Gu, Y.Q., Li, Y.F., Ge, C.C., Zhou, G.Q., Li, B., Zhao, Y.L., Chai, Z.F., Chen, C.Y., 2008. Time-dependent translocation and potential impairment on central nervous system by intranasally instilled TiO2 nanoparticles. Toxicology 254, 82–90.

Warheit, D.B., Webb, T.R., Sayes, C.M., Colvin, V.L., Reed, K.L., 2006. Pulmonary instillation studies with nanoscale TiO2 rods and dots in rats: toxicity is not dependent upon particle size and surface area. Toxicol. Sci. 91, 227–236.

Wing, S.E., Larson, T.V., Hadda, N., Boonyarattaphan, S., Fruin, S., Ritz, B., 2020. Preterm birth among infants exposed to in utero ultrafine particles from aircraft emissions. Environ. Health Perspect. 128.

Yu, L.E., Yung, L.Y.L., Ong, C.N., Tan, Y.L., Balasubramaniam, K.S., Hartono, D., Shui, G. H., Wenk, M.R., Ong, W.Y., 2007. Translocation and effects of gold nanoparticles after inhalation exposure in rats. Nanotoxicology 1, 235–242.

Zhang, J.J., Smith, K.R., 2007. Household air pollution from coal and biomass fuels in China: measurements, health impacts, and interventions. Environ. Health Perspect. 115, 848–855.

Zhang, D.L., Deng, Z.B., Zhang, J.B., Chen, L.Y., 2006. Microstructure and electrical properties of antimony-doped tin oxide thin film deposited by sol-gel process. Mater. Chem. Phys. 98, 353–357.

Zhang, H.-h., Li, Z., Liu, Y., Xinag, P., Cui, X.-y., Ye, H., Hu, B.-l., Lou, L.-p., 2018. Physical and chemical characteristics of PM2.5 and its toxicity to human bronchial cells BEAS-2B in the winter and summer. J. Zhejiang Univ. - Sci. B 19, 317–326.

Zhang, L., Ou, C.J., Magana-Arachchi, D., Vithanage, M., Vanka, K.S., Palanisami, T., Masakorala, K., Wijesekara, H., Yan, Y.B., Bolan, N., Kirkham, M.B., 2021. Indoor particulate matter in urban households: sources, pathways, characteristics, health effects, and exposure mitigation. Int. J. Environ. Res. Publ. Health 18.

Zhao, K.F., Song, Y.Q., Zhang, R.H., Yang, X.Y., Sun, B., Hou, Z.Q., Pu, X.P., Dai, H.X., Bai, X.T., 2019. Comparative toxicity of nanomaterials to air-blood barrier permeability using an in vitro model. Biomed. Environ. Sci. 32, 602–613.